IEEE Access
Multidisciplinary | Rapid Review | Open Access Journal

Received December 21, 2020, accepted January 3, 2021, date of publication January 8, 2021, date of current version January 20, 2021.

*Digital Object Identifier 10.1109/ACCESS.2021.3050340*

# A Novel Sliding-Discrete-Control-Set Modulated Model Predictive Control for Modular Multilevel Converter

**YU JIN[1], QIAN XIAO[2], (Member, IEEE), HONGJIE JIA[2], (Senior Member, IEEE), YUNFEI MU[2], (Member, IEEE), YANCHAO JI[1], TOMISLAV DRAGIČEVIĆ[3], (Senior Member, IEEE), REMUS TEODORESCU[4], (Fellow, IEEE), AND FREDE BLAABJERG[4], (Fellow, IEEE)**

[1]Department of Electrical Engineering and Automation, Harbin Institute of Technology, Harbin 150006, China
[2]Key Laboratory of Smart Grid of Ministry of Education, Tianjin University, Tianjin 300072, China
[3]Center of Electric Power and Energy, Technical University of Denmark, 2800 Lyngby, Denmark
[4]Department of Energy Technology, Aalborg University, 9220 Aalborg, Denmark

Corresponding author: Qian Xiao (xiaoqian@tju.edu.cn)

This work was supported in part by the China Postdoctoral Science Foundation under Grant 2020TQ0222, and in part by the project of the National Natural Science Foundation of China under Grant 52061635103.

**ABSTRACT** Model predictive control (MPC) method has been recognized as one of the most promising technologies for the modular multilevel converter (MMC) due to the fast dynamic response and its simple realization. However, conventional finite control set (FCS) MPC methods for MMC are facing some challenges, such as high computation burden, poor steady-state performance, dependence on weighting factors, and variable switching frequency. In order to solve these problems, a novel sliding-discrete-control-set (SDCS) modulated MPC (MMPC) is proposed for MMC in this paper. Based on the adaptive search step in the output current control, only three control sets are evaluated in each period. In addition, the independent circulating current controller is applied in the proposed MMPC method. With the circulating current controller, the circulating currents are well regulated, and the arm capacitor voltage balancing is realized by circulating current injection. As a result, there is no weighting factor involved in the proposed MMPC method. Compared with the conventional MPC methods, the proposed method obtains a fixed switching frequency in each submodule (SM) and a low comparable computation burden. Simulation and experimental results verify the effectiveness of the proposed method.

**INDEX TERMS** Modular multilevel converter (MMC), high voltage direct current (HVDC), model predictive control (MPC), switching frequency, computation burden.

## I. INTRODUCTION

Nowadays, the modular multilevel converter (MMC) has emerged as one the most popular topologies in various high voltage applications, such as high power direct current (HVDC) power transmission [1], motor drives [2], energy storage system [3], power electronic transformers [4], and so on. Despite its advantages of modularity, flexible scalability, low switching losses, and superior harmonic performance, the conventional cascaded linear control structure in MMC shows a certain limit with the dynamic responses [5]. Therefore, the application of model predictive control (MPC) for MMC has arisen great research interests in recent years.

In [6], a finite control set (FCS) MPC method is proposed for MMC with multiple control targets, including the output current, the circulating current, and the capacitor voltages. Based on the HVDC operation principle, there are $C_{2N}^{N}$ control sets to be evaluated in each period, where $N$ is the number of submodules (SMs) in each arm. The complicated control targets and the huge computation burden limit the application of this basic FCS-MPC method in MMC applications with a high number of SMs. To solve this problem, a series of different methods have been presented. A three-stage FCS-MPC method is proposed in [7], where the output current,

The associate editor coordinating the review of this manuscript and approving it for publication was Chi-Seng Lam.

circulating current, and the capacitor voltages are predicted and controlled separately. The number of evaluated control sets is slightly reduced. By taking the inserted SM numbers in the upper arm and the lower arm as two independent variables in the basic control sets, the number of the evaluated control sets is reduced from $C_{2N}^{N}$ to $(N+1)^2$ in [8]. The number of evaluated control sets is further decreased by allocating SfMs in the same arm into several different groups [9]. And the optimization of the grouping configuration is also discussed by a series of simulation results in [10].

A two-stage MPC method is proposed in [11], where $(N+1)$ control sets are evaluated in each period. However, the second-order circulating current is not well-suppressed according to the experimental results. *P. Guo et al.* propose an MPC method with a reduced calculation burden by search space optimization, and the circulating current is also well controlled with the two-stage control method [12]. In [13], a fast MPC is proposed with three evaluated control sets to limit the voltage and the current ripple, and the capacitor voltage balancing is realized by sorting method. This method avoids the prediction of the capacitor voltages, and the calculation amount thus decreases. A group-sorting is further applied in the MPC method, and the computation burden is thus reduced [14]. In addition, the uncontrolled common-mode voltage can endanger the power converters under specific operations [15]. To avoid this issue, the common-mode voltage is injected and regulated in the MPC method to suppress the circulating currents and reduce capacitor voltage ripples at the same time [16]. However, this method generates only $(N+1)$ output voltage levels. To increase the output voltage levels, output voltage level (OVL) based MPC is proposed in [17] with $2N+1$ output voltage levels. However, the one-stage predictive control method requires a large calculation amount. By preselecting output voltage levels of each arm, the MPC method with $2N+1$ output voltage levels is improved in [18], where five control sets are evaluated in each period. Based on this, another improved method is proposed by preselecting according to the circulating current, and there are only three control sets evaluated in each period [19]. The above FCS-MPC methods have the inherent advantages of fast dynamic response, multiple control targets, and easy realization. However, the above MPC methods have a variable switching frequency, and they require a large amount of calculation.

A modulated model predictive control (MMPC) method is proposed for MMC in voltage source converter (VSC) HVDC application in [20]. This method is designed by controlling the duty cycle instead of controlling the switching signals or output voltage levels presented in the above FCS-MPC methods. Moreover, this method includes a two-step duty cycle calculation. The first duty cycle is designed for the two selected optimal vectors to control the output currents. The second duty cycle is designed for circulating current control. However, the sorting-based capacitor voltage balancing method cannot guarantee fixed switching frequency in each SM, and the circulating currents are not well suppressed. *D. Zhou et al.* propose a two-stage MMPC method with carrier-phase-shift (CPS) PWM [21]. This method considers the arm voltage as a whole and preselects the arm voltage vectors based on the predicted output currents. With the two selected vector, the second prediction stage further determines the optimal duty cycle. Therefore, the duty cycle calculation is simplified. To avoid the complicated two-stage prediction and duty cycle calculation, *J. Wang et al.* propose a deadbeat predictive current control method [22], where the modulation references for each arm are calculated directly based on the output current references and measured values. This method provides a fixed switching frequency for each SM. However, there is no cost function involved in this deadbeat based predictive control method, which limits its application in the multi-target control situation. Recently, the MPC method with the adaptive search step is applied in DC microgrids aiming to solve the dynamic response issues brought by the pulse loads [23], [24]. By applying the adaptive search step in the MPC algorithm, the evaluated control sets can be reduced accordingly.

Based on the above-mentioned issues and existing methods, this paper proposes a novel sliding-discrete-control-set (SDCS) modulated model predictive control (SDCS-MMPC) for the modular multilevel converter. The main characteristics of the proposed method are listed below.

1) The sliding-discrete-control-set is applied in the MMPC method in MMC, where only three control sets are evaluated in each period. Hence, a low computation burden is obtained.

2) The proposed SDCS-MMPC method obtains a fixed switching frequency in each SM by CPS-PWM, and the switching loss in each SM is thus more evenly distributed.

3) The proposed method realizes DC capacitor voltage balancing between the upper and the lower arms by injection of the fundamental-frequency circulating currents. Therefore, the arm capacitor voltage in cost function ([6]) is eliminated.

4) The circulating current controller is disintegrated from the cost function of the MPC algorithm in this paper. The independent control structure leads to better control of the circulating currents compared with the MMPC method in [20].

The rest of the paper is outlined as follows. Section II introduces the model and an example of the existing MMPC method. The detailed principle of the proposed SDCS-MMPC and comparison are described in Section III. Simulation results in Section IV and experimental results in Section V verify the effectiveness of the proposed method. The conclusions are listed in Section VI.

## II. EXISTING MMPC METHOD

### A. TOPOLOGY AND MODEL OF MMC

The topology of the three-phase half-bridge (HB) MMC is shown in Fig. 1. The MMC consists of three identical phase legs, each of which includes the upper arm and the lower arm. In each arm, there are $N$ identical HB SMs. The upper arm and the lower arm in the phase leg are connected as the output terminal through two arm inductors, $L_{arm}$. By an additional

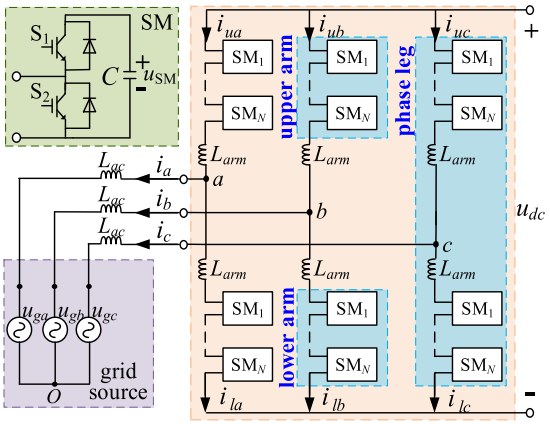


**FIGURE 1.** The topology of MMC.

AC filter inductor, $L_{ac}$, the output terminal is connected to the AC grid. The structure of each HB SM is also shown in Fig. 1, where there are two power switches in HB connection and one capacitor. Supposing the capacitor voltage of the SM is $u_{\mathrm{SM}}$, the output voltage of the HB SM is $u_{\mathrm{SM}}$ if it is inserted, while the output voltage is 0 if it is bypassed.

To realize precise control of MMC, a single-phase model of MMC is shown in Fig. 2. The equivalent circuit of MMC includes two parts, the AC path and the DC path. The AC path can be applied to control the output currents of MMC, while the DC path can be applied to control the circulating currents.

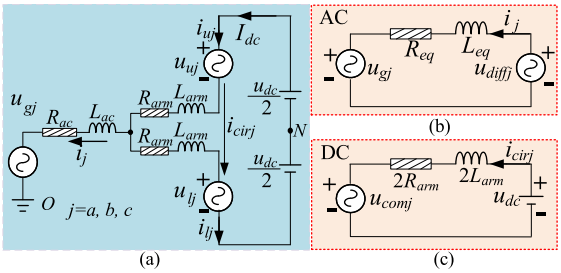


**FIGURE 2.** Equivalent circuit of MMC. (a). Single-phase model of MMC. (b). AC path model. (c). DC path model.

The AC control path can be simplified as Fig. 2 (b), the mathematical model of which can be expressed as

$$\begin{cases} R_{eq} i_j + L_{eq} \dfrac{di_j}{dt} = u_{diffj} - u_{gj} \\ i_j = i_{uj} - i_{lj},\ u_{diffj} = \dfrac{u_{lj} - u_{uj}}{2} \end{cases} \tag{1}$$

where $i_j$ $(j = a, b, c)$ is the output current of MMC; $i_{uj}$ and $i_{lj}$ are the arm currents of the upper and the lower arm; $u_{gj}$ is the grid voltage; $u_{uj}$ and $u_{lj}$ are the arm voltages of the upper and the lower arm; $R_{eq}$ and $L_{eq}$ are the equivalent resistance and inductance in the equivalent circuit of the AC control loop, which can be expressed as

$$R_{eq} = R_{ac} + R_{arm}/2, \quad L_{eq} = L_{ac} + L_{arm}/2 \tag{2}$$

where $L_{arm}$ and $R_{arm}$ are the inductances and resistances of the arm inductor; $L_{ac}$ and $R_{ac}$ are the inductances and resistances of the AC filter inductor.

The DC control path can be simplified as Fig. 2 (c), the mathematical model of which can be expressed as

$$\begin{cases} 2R_{arm} i_{cirj} + 2L_{arm} \dfrac{di_{cirj}}{dt} = u_{dc} - u_{comj} \\ i_{cirj} = \dfrac{(i_{uj} + i_{lj})}{2},\ u_{comj} = u_{lj} + u_{uj} \end{cases} \tag{3}$$

where $i_{cirj}$ is the circulating current; $u_{dc}$ is the DC side voltage of MMC; $i_{uj}$ and $i_{lj}$ are the arm current of the upper and the lower arm.

### B. THE EXISTING MMPC METHOD

For the existing MMPC method, the first step is to choose the optimal vectors among all the possible control sets. Then, based on the selected optimal control sets, the duty cycle of these vectors in each period is calculated to precisely track the output current reference [20], [21]. In this paper, considering its more general operation process and duty cycle calculation method, reference [20] is introduced as an example of the existing MMPC to make a comparison with the proposed SDCS-MMPC method.

This method includes two steps. The first step is to select the two optimal control sets and calculate the duty cycles of them. The second step is to calculate the duty cycle used for the circulating current controller. The basic principle is shown in Fig. 3.

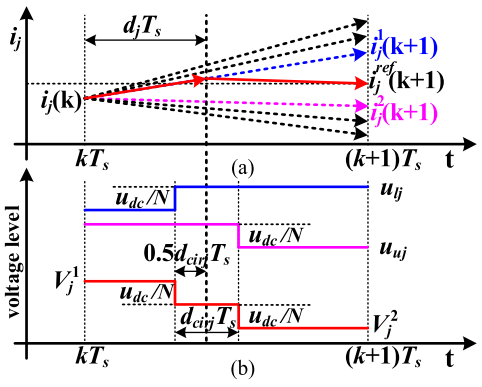


**FIGURE 3.** The basic principle of the MMPC method in [20]. (a). The principle of the first step. (b) The basic principle of the second step supposing the circulating current is higher than the reference.

For the first step, the basic principle is shown in Fig. 3 (a). $(N + 1)$ control sets are evaluated during this process, and they can be expressed as

$$V_j = (N_{uj}, N_{lj}) \in \{(N, 0), (N-1, 1), \ldots (1, N-1), (0, N)\} \tag{4}$$

where $N_{uj}$ and $N_{lj}$ are the numbers of the inserted SM in the upper and the lower arm.

Based on (1) to (3), the discrete mathematic control model of the output current can be expressed as

$$\begin{cases} i_j(k+1) = A[u_{lj}(k) - u_{uj}(k) - 2u_{gj}(k)] + Bi_j(k) \\ A = \dfrac{T_s}{2L_{ac} + L_{arm}},\ B = 1 - \dfrac{(R_{arm} + R_{ac})T_s}{2L_{ac} + L_{arm}} \end{cases} \tag{5}$$

where $T_s$ is the sampling period; $i_j(k+1)$ is the predicted output current at $k+1$ time instant; $u_{gj}(k)$ is the measured grid voltage at $k$ time instant; $i_j(k)$ is the measured output current at $k$ time instant; $u_{uj}(k)$ and $u_{lj}(k)$ are the arm voltages of the upper and the lower arm at $k$ time instant, which are expressed as

$$u_{uj}(k) = \frac{N_{uj}}{N}(k)V_{uj}, \quad u_{lj}(k) = \frac{N_{lj}}{N}(k)V_{lj} \tag{6}$$

where $V_{uj}$ and $V_{lj}$ are the sums of the SM capacitor voltages in the upper and the lower arm.

With the output current predicted by equation (5) and (6), two optimal control sets will be selected based on the cost function

$$J_{\mathrm{MMPC1}}(k+1) = |i_j^{ref}(k+1) - i_j(k+1)| \tag{7}$$

According to the cost function in (7), two optimal control sets with two minimum values of the cost function are selected and recorded as $V_j^1$ and $V_j^2$. The duty cycle of the two selected control sets can be expressed as

$$d_j = \frac{i_j^{ref}(k+1) - i_j^1(k+1)}{i_j^1(k+1) - i_j^2(k+1)} \tag{8}$$

where $i_j^1(k+1)$ and $i_j^2(k+1)$ are the predicted output currents under control sets $V_j^1$ and $V_j^2$.

For the second step, the basic principle is shown in Fig. 3 (b). Three control sets are evaluated during this process, and they are expressed as

$$\begin{cases} V_{cirj} = N_{uj} + N_{lj} \in \{N-1, N+1\} \\ V_{cirj}^0 = N_{uj} + N_{lj} = N \end{cases} \tag{9}$$

Based on (1) to (3), the discrete mathematic model can be derived, and the predicted circulating currents can be expressed as

$$\begin{cases} i_{cirj}(k+1) = C[u_{dc} - (u_{lj}(k) + u_{uj}(k))] + Di_{cirj}(k) \\ C = \dfrac{T_s}{2L_{arm}},\ D = 1 - \dfrac{R_{arm}T_s}{L_{arm}} \end{cases} \tag{10}$$

where $i_{cir}(k+1)$ is the predicted circulating current at $k+1$ time instant; $i_{cirj}(k)$ cannot be measured directly, and it is calculated by the two other measured variables according to the equation $i_{cirj} = (i_{uj} + i_{lj})/2$.

Based on the predicted value and measured value of the circulating current, $V_{cirj}^0$ and are selected, together with another one of the other two control sets in $V_{cirj}$, which is recorded as $V_{cirj}^1$. The duty cycle of the two selected control sets can be expressed as

$$d_{cirj} = \frac{i_{cirj}^{ref}(k+1) - i_{cirj}^0(k+1)}{i_{cirj}^1(k+1) - i_{cirj}^0(k+1)} \tag{11}$$

where $i_{cirj}^1(k+1)$ and $i_{cirj}^0(k+1)$ are the predicted output currents under the control sets of $V_{cirj}^1$ and $V_{cirj}^0$.

With the selected control sets and the calculated duty cycles $d_j$ and $d_{cirj}$, the MMC can be controlled according to the principle in Fig. 3 (b). However, this MMPC method can still be improved by the following aspects.

1) There are $N+4$ evaluated control sets in each phase within each period, and the two-step duty cycle calculation is required. Both processes increase the computation burden of the control system.

2) The sorting based modulation method is applied for the capacitor voltage balancing in [20]. The cost function is simplified without capacitor voltage predictions. However, this voltage balancing process introduces a variable switching frequency in each SM.

3) Only one additional SM is utilized for the circulating current regulation. Therefore, the suppression capability of the circulating current is limited, and the second-order circulating current cannot be ideally suppressed according to the results in [20].

## III. THE PROPOSED SDCS-MMPC METHOD

### A. THE OVERALL CONTROL DIAGRAM

In this paper, an SDCS-MMPC method is proposed to solve the above-mentioned issues in the existing MMPC method. As shown in Fig. 4, three individual parts are included in the proposed method, the SDCS-MMPC output current control, the arm energy and the circulating current control, and the modulation scheme.

The SDCS-MMPC output current control is applied to control the output currents. $u_{ujm}(k)$ and $u_{ljm}(k)$ are the measured capacitor voltages in the upper and the lower arm at $k$ time instant, where $j = a, b, c$, and $m = 1, 2, \ldots N$; $u_{gj}(k)$ and $i_j(k)$ are the measured grid voltage and the measured output current at $k$ time instant; $i_j(k+1)$ is the predicted output current at $k+1$ time instant; $i_j^{ref}(k)$ and $i_j^{ref}(k+1)$ are the reference value of $i_j^{ref}$ at $k$ and $k+1$ time instant; $\Delta_v$ is the adaptive search step in the proposed algorithm; $J(k+1)$ is the cost function at $k+1$ time instant; $v_{oj}$ is the optimal output voltage reference.

The arm energy and circulating current control is designed to control the average capacitor voltage in each arm by circulating current injection. $V_{uj}$ and $V_{lj}$ are the sums of the SM capacitor voltages in the upper and the lower arm; $u_{dc}$ is the DC side voltage of MMC; $\theta$ is the phase angle of the grid voltages; $P$ is the active power in the AC side; $v_{cirj}$ is the voltage references generated by the circulating current controller.

The CPS-PWM is applied as the modulation scheme, where a fixed switching frequency is obtained in each SM. $n_{ujm}$ and $n_{ljm}$ are the final modulation references of each SM in the upper and the lower arm. The detailed information about SM capacitor voltage balancing and CPS-PWM scheme can be found in [25], and it will not be discussed in this paper.

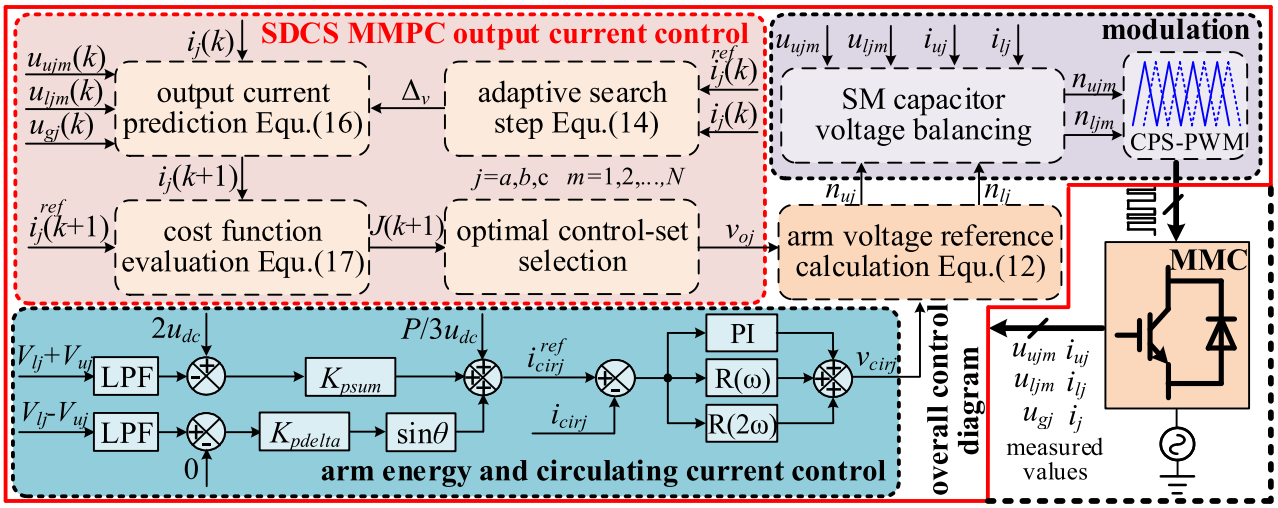


**FIGURE 4.** The overall control diagram of the proposed SDCS-MMPC method.

In addition, it is noted that based on $v_{oj}$ and $v_{cirj}$, the modulation references for the upper arm and the lower arm can be expressed as

$$n_{uj} = \frac{1}{2} - \frac{v_{oj}}{V_{uj}} + \frac{v_{cirj}}{V_{uj}}, \quad n_{lj} = \frac{1}{2} + \frac{v_{oj}}{V_{lj}} + \frac{v_{cirj}}{V_{lj}} \tag{12}$$

where $n_{uj}$ and $n_{lj}$ are modulation references of the upper and the lower arm.

More details will be discussed in subsections B and C.

### B. THE PROPOSED SDCS_MMPC OUTPUT CURRENT CONTROL

#### 1) THE BASIC PRINCIPLE OF SDCS-MMPC

The basic flowchart of the proposed SDCS-MMPC method is shown in Fig. 5. Firstly, the adaptive search step $\Delta_v$ is configured according to the difference between the output current reference and its measured value. Then, the three evaluated control sets for the current time instant is decided based on $\Delta_v$. Next, the output current is predicted, and the cost function is evaluated for each control set according to the MMC model and the measured variables. Finally, the optimal control set is selected among the three control sets based on the calculated cost function.

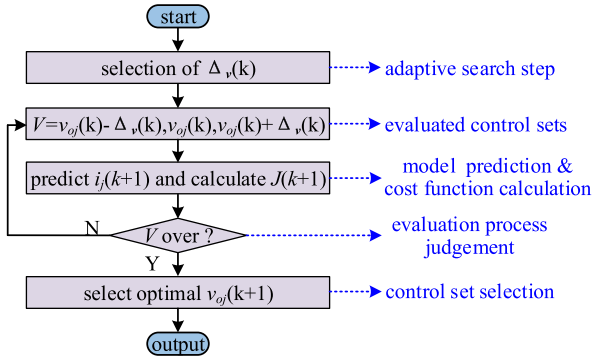


**FIGURE 5.** The flowchart of the proposed SDCS-MMPC method.

#### 2) THE ADAPTIVE SEARCH STEP AND THE EVALUATED CONTROL SETS

For the proposed method, the sliding discrete control sets are applied, which means the optimal control set from the last time constant is recorded and reapplied as one of the evaluated control sets at the next time instant. As a result, only three control sets are evaluated in each period, which is independent of the number of SMs in each arm. The fundamental variable in the control set is $v_{oj}$, and the evaluated control sets can be expressed as

$$V = [v_{oj}(k) - \Delta_v(k), \quad v_{oj}(k), \quad v_{oj}(k) + \Delta_v(k)] \tag{13}$$

For this SDCS-MMPC method, a larger search step $\Delta_v$ improves the dynamic response of the system, but it also deteriorates the steady performance and increases the system oscillation around the steady-state operation point. Therefore the adaptive search step $\Delta_v$ should be empirically tuned to obtain a suitable dynamic response as well as a good steady-state performance. In this paper, the adaptive search step is selected based on the following principle

$$\Delta_v(k) = \begin{cases} E_{up}, & \zeta E_i > E_{up} \\ \zeta E_i, & E_{low} < \zeta E_i < E_{up} \\ E_{low}, & \zeta E_i < E_{low} \end{cases} ; \quad E_i = \frac{|i_j^{ref}(k) - i_j(k)|}{I_{ref}(k)} \tag{14}$$

where $I_{ref}$(k) is the amplitude of the output current at $k$ time instant; $E_i$ is the normalized value of the current differences between the reference and the real-time value; $E_{up}$ and $E_{low}$ are the upper and the lower limit for the adaptive search step selection; $\zeta$ is the empirical parameter. In this paper, $\zeta$ is selected as $u_{dc}/2$; $E_{up}$ and $E_{low}$ are selected as $0.1u_{dc}$ and $0.005u_{dc}$. A similar parameter design principle for the

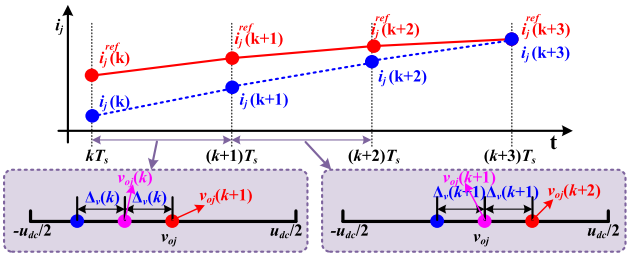


**FIGURE 6.** The working principle of the proposed SDCS-MMPC method.

adaptive search step can be found in [23], and this is not discussed here.

#### 3) THE OUTPUT CURRENT PREDICTION AND THE COST FUNCTION

With the above determined evaluated control sets, the output current can be predicted based on the discrete MMC model in (5).

According to (12), $v_{oj}$ can be expressed as

$$v_{oj}=\frac{n_{lj}V_{lj}-n_{uj}V_{uj}}{2}=\frac{u_{lj}-u_{uj}}{2},\quad v_{oj}\in\left(-\frac{u_{dc}}{2},\frac{u_{dc}}{2}\right) \tag{15}$$

Substituting equation (15) into (5), the output current can be predicted as

$$i_j(k+1)=A[2v_{oj}(k)-2u_{gj}(k)]+Bi_j(k) \tag{16}$$

where $A$ and $B$ are the same as in (5). And the final cost function can be expressed as

$$J(k+1)=|i_j^{ref}(k+1)-i_j(k+1)| \tag{17}$$

where $i_j^{ref}(k+1)$ is the output current reference at $k+1$ time instant. Based on Lagrange third-order extrapolation method [22], it can be expressed as

$$i_j^{ref}(k+1)=4i_j^{ref}(k)-6i_j^{ref}(k-1)+4i_j^{ref}(k-2)-i_j^{ref}(k-3) \tag{18}$$

where $i_j^{ref}(k)$, $i_j^{ref}(k-1)$, $i_j^{ref}(k-2)$, and $i_j^{ref}(k-3)$ are the output current reference at $k$, $k-1$, $k-2$, and $k-3$ time instant.

By (16) and (17) the cost function under each control set can be evaluated, and the optimal control set for the next time instant can be selected.

Based on the above description, the working principle of the proposed MMPC can be further illustrated in Fig. 6. Supposing the optimal control set at $k$ time instant is $v_{oj}$(k), and the output current is lower than the reference value. Then, the control sets around $v_{oj}$(k) will be evaluated, and the optimal control set for $k+1$ time instant will be $v_{oj}$(k+1) = $v_{oj}$(k)+$\Delta_v$(k). With the selected optimal control set, the output current is lower than the reference value. Again, the control sets around $v_{oj}$(k+1) will be evaluated, and the optimal control set for $k+2$ time instant will be $v_{oj}$(k+2)= $v_{oj}$(k+1)+$\Delta_v$(k+1).

### C. THE CIRCULATING CURRENT CONTROL

For the proposed method, the references of the circulating current include three parts, and the capacitor voltage balancing between different arms is realized by fundamental-frequency circulating current injection. The first two parts are applied to control the voltage sum of the two arms and the voltage difference between the two arms. The third part is obtained by power feed-forward from the AC side. More information about the references can be found in [24], and the final circulating current references can be expressed as

$$i_{cirj}^{ref}=K_{psum}(2u_{dc}-V_{uj}-V_{lj})+K_{pdelta}(V_{lj}-V_{uj})\cos\theta_j+i_{dc} \tag{19}$$

where $i_{dc}$ can be expressed as $i_{dc}=P/3u_{dc}$; $\theta_j$ is the phase angle of the grid voltage.

For the MMPC method in [20], when the output voltage reference is determined, the circulating current is controlled by adjusting the redundant switching status, where only two SMs are involved at most. Therefore, the effectiveness of the circulating current control is limited.

To realize the individual and precise control of the circulating current, a conventional PIR controller is applied in this paper. The voltage references for the circulating current control, $v_{cirj}$, can be derived as

$$v_{cirj}(k)=(K_{p1}+\frac{K_{i1}}{s}+\frac{K_{R1}ws}{s^2+ws+w^2}+\frac{2K_{R2}ws}{s^2+2ws+(2w)^2})(i_{cirj}^{ref}-i_{cirj}) \tag{20}$$

With the independent circulating current controller, the circulating current can be regulated.

### D. COMPARISON

To better elaborate, the characteristics of the proposed SDCS-MMPC method, a series of detailed comparisons with different MPC methods are listed in Table 1.

For the evaluated control sets in each period, the number of conventional FCS-MPC methods usually varies from $C_{2N}^{N}$ to 3, while the number of the proposed method in each period is only three. In addition, the proposed method has the $2N+1$ output voltage levels, while some of the conventional FCS-MPC methods only have the $N+1$ output voltage levels. Moreover, the proposed method obtains a fixed switching frequency in each SM, while the conventional FCS-MPC methods have variable switching frequencies in each SM.

Compared with the MMPC methods, the proposed method requires no vector selection and the duty cycle calculation, which leads to a simplified control structure. In addition, the circulating current is controlled individually, and there are no weighting factors involved in the cost function. This process leads to better performance on the circulating current and easier design of the control parameters.

It is noted that the proposed MMPC method includes the output current $i_j$ as the only control target in the cost function, and it requires a proper selection of the adaptive search step.

**TABLE 1. Comparison of different MPC control methods.**

| Methods | FCS-MPC [6] | FCS-MPC [8] | FCS-MPC [11] | FCS-MPC [13] | Preselecting MPC [18] | Preselecting MPC [19] | MMPC [20] | MMPC [21] | **Proposed Method** |
|---|---|---|---|---|---|---|---|---|---|
| evaluated control sets/per phase | $C_{2N}^{N}$ | $(N+1)^2$ | $(N+1)$ | 3*3 | 5 | 3 | $(N+4)$ | 4 | **3** |
| Duty cycle calculation | No | No | No | No | No | No | Yes | Yes | **No** |
| No. of output voltage levels | $N+1$ | $2N+1$ | $N+1$ | $N+1$ | $2N+1$ | $2N+1$ | $2N+1$ | $2N+1$ | **$2N+1$** |
| SM switching frequency | Variable | Variable | Variable | Variable | Variable | Variable | Variable | Fixed | **Fixed** |
| Multiple weighting factors | Yes | Yes | No | No | Yes | Yes | Yes | Yes | **No** |
| Individual control ($i_j$ and $i_{cirj}$) | No | No | Yes | Yes | No | No | No | No | **Yes** |
| Three-phase application | Yes | Yes | Yes | Yes | Yes | Yes | Yes | No | **Yes** |
| $i_{cirj}$ control and second-order suppression effect | Not well-controlled | Well-controlled | Not controlled | Well-controlled | Well-controlled | Well-controlled | Not totally suppressed | Well-controlled | **Well-controlled** |
| Dynamic response | Fast | Fast | Fast | Compromise with $i_j$ ripple | Fast | Fast | Fast | Fast | **Fast** |
| Multiple control targets in MPC | Yes | Yes | Yes | Yes | Yes | Yes | Yes | Yes | Only $i_j$ |
| Adaptive search step design | No | No | No | No | No | No | No | No | Yes |

In order to better analyze the computation burden of the proposed method, the comparisons with some MPC methods are further carried out. According to reference [26], the complexity of an algorithm can be stated by the estimation of the required runtime. For the estimated real-time execution time, it can be expressed as

$$t_{real} = \psi_{run} T_{cycle} \tag{21}$$

where $t_{real}$ is the estimated real-time of the controller; $\Psi_{run}$ is the number of the runtime cycles of these algorithms; $T_{cycle}$ is the execution time of the basic operation cycle.

Considering that different operations (such as addition, multiplication, absolute, and so on) require different runtime cycles, the required runtime for the common basic operations can be defined as in Table 2, which are listed based on the similar computation burden estimation method in [27]. With the definition in Table 2, the required runtime, and the complexity of the MPC algorithms are listed in Table 3. It can be seen that the proposed method has an advantage in its computation burden.

**TABLE 2. Runtime of different basic operations.**

| Basic operations | Run cycles $\Psi_{run}$ | Basic operations | Run cycles $\Psi_{run}$ |
|---|---|---|---|
| Addition | 1 | Multiplication | 1 |
| Assignment | 1 | Absolute | 2 |
| Look-up | 1 | Comparison | 1 |

## IV. SIMULATION RESULTS

A three-phase MMC model is built in the MATLAB/SIMULINK environment to verify the effectiveness and the characteristics of the proposed SDCS-MMPC method. The simulation parameters can be found in Table 2, which are selected according to references [24]. To better demonstrate the advantages of the proposed method, comparison results between the conventional MMPC method [20] and the proposed method are given in Fig. 7 and Fig. 8.

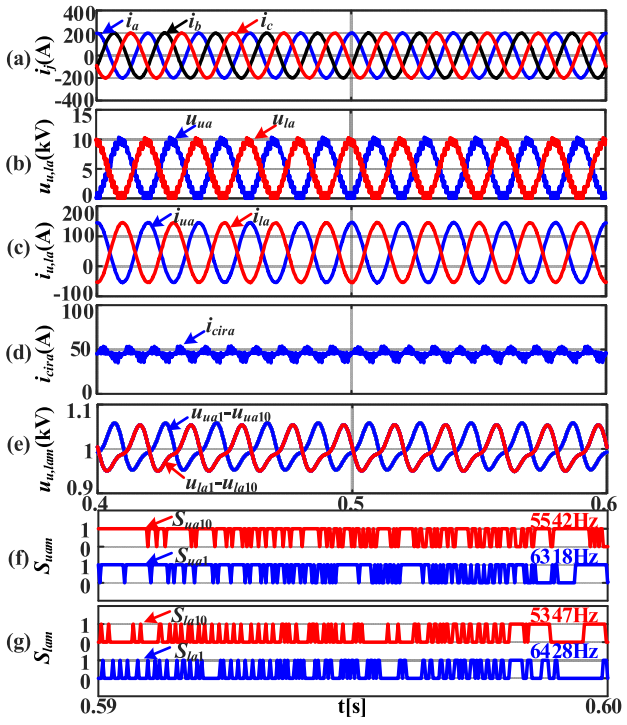


**FIGURE 7. Simulation results of the steady-state performance with the conventional MMPC method in [20]. (a). Output currents. (b). Output arm voltages. (c). Arm currents. (d). Circulating current. (e). Capacitor voltages. (f). Switching signals. (g). Switching signals.**

### A. STEADY-STATE PERFORMANCE

The steady-state performance of the conventional MMPC method is shown in Fig. 7, where the rated output current of MMC is set as 200 A. As is shown in Fig. 7 (a), the amplitude

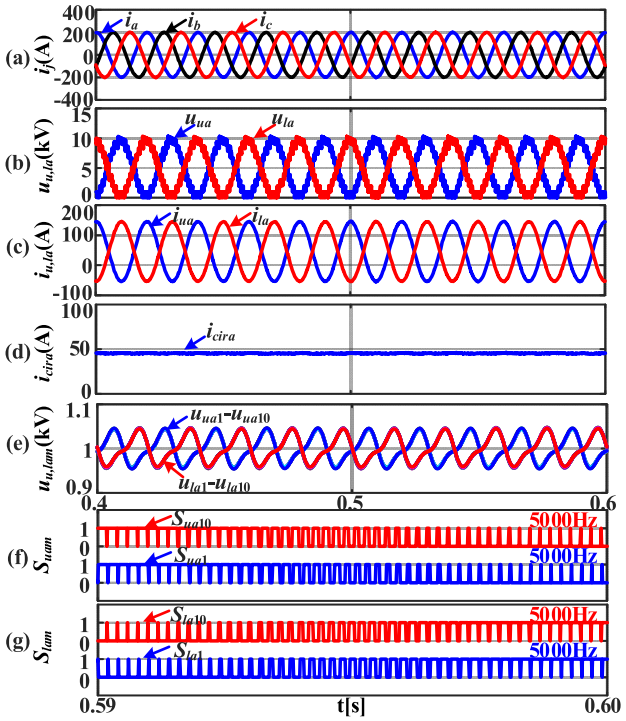


**FIGURE 8.** Simulation results of the steady-state performance with the proposed method. (a). Output currents. (b). Output arm voltages. (c). Arm currents. (d). Circulating current. (e). Capacitor voltages. (f). Switching signals. (g). Switching signals.

of the output current in MMC is 200 A, which is the same as the preset value. Fig. 7 (b) shows the output voltage of the upper and the lower arm, where the maximum value is almost equal to 10 kV, the voltage of the DC side. The arm currents are shown in Fig. 7 (c), where the peak-peak value is about 200 A, and the DC offset is about 45 A. The circulating current of the conventional method is given in Fig. 7 (d), where the average value is about 45 A. However, it can be clearly seen that the second-order circulating current is not well suppressed. Fig. 7 (e) shows the capacitor voltages, where the average value is about 1 kV. Fig. 7 (f) and Fig. 7 (g) give the switching signals of four random SMs in phase A ($SM_1$ and $SM_{10}$ in the upper arm, $SM_1$ and $SM_{10}$ in the lower arm). The switching frequencies of the four SMs are variable, about 5542 Hz, 6318 Hz, 5347 Hz, and 6428 Hz, respectively.

The steady-state performance of the proposed SDCS-MMPC is shown in Fig. 8, where the rated output current of MMC is also set as 200 A. As is shown in Fig. 8 (a), the amplitude of the output current in MMC is the same as 200 A, the preset value. Fig. 8 (b) shows the output voltage of the upper and the lower arm, where the maximum value is about 10 kV, equal to the voltage of the DC side. The arm currents are shown in Fig. 8 (c), where the peak-peak value is about 200 A, and the DC offset is about 45 A. The circulating current of the proposed method is given in Fig. 8 (d), where the average value is about 45 A. In addition, compared with that of the conventional method in Fig. 7 (d), the proposed method shows a better performance in the circulating current suppression. Fig. 8 (e) shows the capacitor voltages, where the average value is about 1 kV. Fig. 8 (f) and Fig. 8 (g) give the switching signals of four random SMs in phase A ($SM_1$ and $SM_{10}$ in the upper arm; $SM_1$ and $SM_{10}$ in the lower arm). The switching frequencies of the four SMs are all fixed at 5 kHz.

The above simulation results show the effectiveness of the proposed method. Compared with the conventional MMPC method, the proposed method obtains a better steady-state performance in circulating current control. In addition, the proposed method obtains a fixed switching frequency in each SM, which leads to an evenly distributed switching loss.

### B. INFLUENCE OF CONTROL PARAMTERS IN MMPC ALGORITHM

To explore the influence of the control parameters in the proposed MMPC method on the steady-state performance, a series of simulations are carried, and the influence on output current THD and the rising time is shown in Fig. 9. In Fig. 9, $\zeta$ is defined in (14); $\mu$ is the search range of the proposed MMPC. Since the output current is AC component, the rising time is defined as

$$t_{rise} = t_{5\%error} - t_{95\%error} \tag{22}$$

where $t_{5\%error}$ and $t_{95\%error}$ are the time when the error between the output current and its reference value is 5% and 95%.

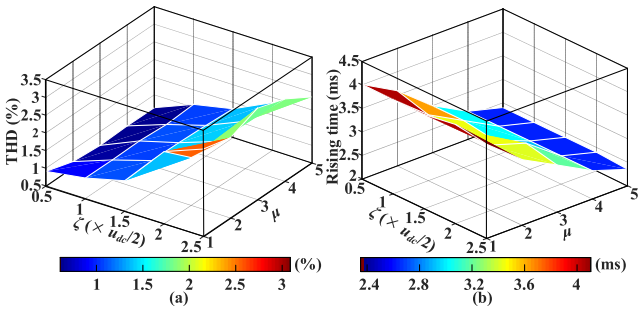


**FIGURE 9.** The influence of the proposed MMPC control variables on steady-state performance. (a). The relation curve of output current THD. (b). The relation curve of the rising time.

It is noted that $\mu$ directly decides the evaluated control sets in each period. For example, when $\mu = 1$, there are 3 control sets evaluated; when $\mu = x$, there are $2x+1$ evaluated control sets in each period. As shown in Fig. 9 (a), when $\zeta$ is selected between 0.5 (pu) to 1.5 (pu), the THD of output current is mainly influenced by $\zeta$, and it is almost proportional to $\zeta$; when $\zeta$ is higher than 1.5 (pu), the THD is influenced by both $\zeta$ and $\mu$. According to Fig, 9 (b), for the proposed method, the rising time is mainly decided by the search range $\mu$, and it is almost in inverse ratio to $\mu$. However, the calculation burden will increases significantly with the increase of $\mu$.

With due consideration based on the curve in Fig. 9, the final $\zeta$ is selected as 1 (pu), and $\mu$ is selected as 1.

**TABLE 3.** Runtime and time complexity of MPC algorithms.

| MPC algorithms | | Run cycles / phase $\Psi_{run}$ | Time complexity |
|---|---|---|---|
| Switching status based FCS-MPC [6] | | $(5N+12)C_{2N}^{N}-1$ | $O(C_{2N}^{N})$ |
| Inserted SM No. based FCS-MPC [8] | | $161N^2+321N+160$ | $O(N^2)$ |
| Output voltage level based dual-stage FCS-MPC [11] | | $0.5(1+C_N^{[0.5N]})+14N$ + 20 (in average) | $O(C_N^{[0.5N]})$ |
| Arm voltage level based FCS-MPC [13] | | $N^2+37N+294$ | $O(N^2)$ |
| Preselection based FCS-MPC [18] | | $N^2+N+246$ | $O(N^2)$ |
| Preselection based FCS-MPC [19] | | $N^2+N+120$ | $O(N^2)$ |
| Preselected two-stage based MMPC [20] | | $N^2+28N+68$ | $O(N^2)$ |
| Duty cycle calculated MMPC [21] | | $12N+136$ | $O(N)$ |
| **Proposed method** | $M^2PC$ current control | 56 | $O(N)$ |
| | circulating current control | 39 | |
| | individual voltage balancing | $8N+3$ | |
| | total | $8N+98$ | |

Therefore, only three control sets are evaluated in each sampling period.

## V. EXPERIMENTAL RESULTS

In order to further verify the effectiveness and the dynamic response of the proposed method, experiments are conducted on a three-phase laboratory prototype. The prototype is shown in Fig. 10. The experiment parameters are also listed in Table 4. The prototype works in inverter mode, and the output terminals of the converter are connected to a three-phase programmable AC source. The dSPACE 1006 works as the central controller, and PSS15S92F6-AG, the intelligent power module, works as the main power switch. It is noted to realize the delay compensation for the real-time experimental results, a two-step ahead prediction is applied in this paper.

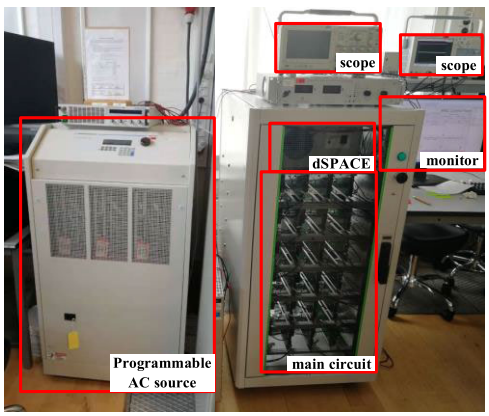


**FIGURE 10.** The prototype of the three-phase down-scaled MMC.

The steady-state performance of the proposed method is shown in Fig. 11 and Fig. 12, where the amplitude of the output currents for MMC is set as 4 A. As shown in Fig. 11 (a), the amplitude of the output currents is about 4 A. The output arm voltages of the upper arm and the lower arm in phase *A* are shown in Fig. 11 (b), the maximum value of which is close

**TABLE 4.** Validation System Parameters.

| Items | | Symbols | Simulations | Experiments |
|---|---|---|---|---|
| Grid line voltage | | $v_{gl}$ | 5.5 kV | 105 V |
| Rated DC voltage | | $u_{dc}$ | 10 kV | 200 V |
| Rated power | | $S_{rated}$ | 2 MVA | 1200 VA |
| Arm inductor | inductance | $L_{arm}$ | 5 mH | 10 mH |
| | resistance | $R_{arm}$ | 0.1571 Ω | 1.2 Ω |
| AC inductor | inductane | $L_{ac}$ | 3.85 mH | 1.8 mH |
| | resistance | $R_{ac}$ | 0.1210 Ω | 0.26 Ω |
| Carrier frequency | | $f_{carrier}$ | 5 kHz | 2000 Hz |
| SM number per arm | | $N$ | 10 | 4 |
| SM capacitance | | $C$ | 2 mF | 1.8 mF |
| Other control paras | circulating current control | $K_{p1}$, $K_{i1}$ | 100, 10 | 20, 40 |
| | | $K_{R1}$ | 200 | 400 |
| | | $K_{R1}$ | 400 | 800 |
| | individual voltage control | $K_{p\_indi}$ | 0.01 | 0.005 |

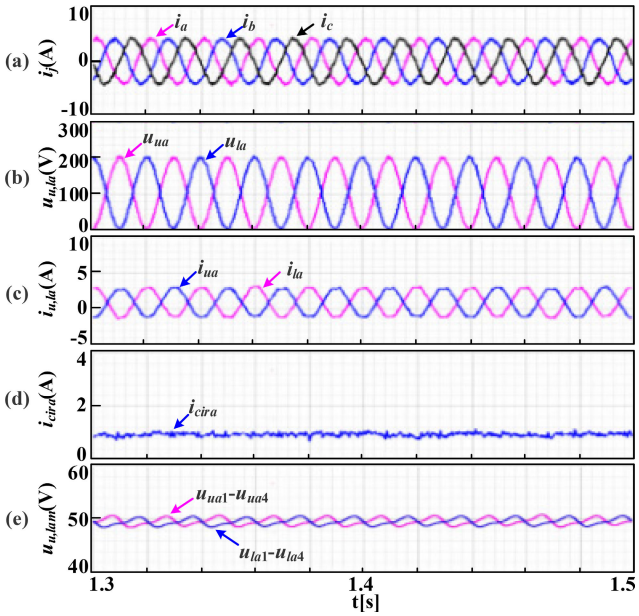


**FIGURE 11.** Experimental steady-state performance of the proposed method. (a). Output currents. (b). Output arm voltages. (c). Arm currents. (d). Circulating current. (e). Capacitor voltages.

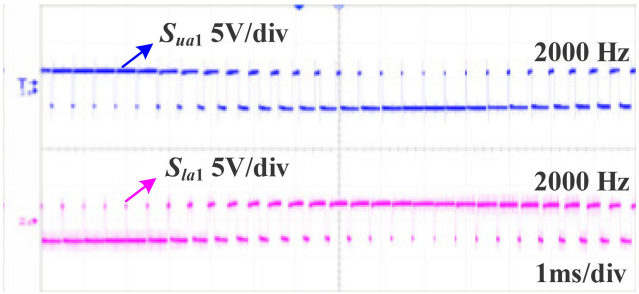


**FIGURE 12.** Switching signals of the experimental steady-state performance of the proposed method.

to the DC voltage 200 V. Fig. 11 (c) shows the arm currents of the upper arm and the lower arm in phase *A*. The circulating current in phase *A* is shown in Fig. 11 (d), where the circulating current is well suppressed. The capacitor voltages are shown in Fig. 11 (e), which are about 50 V. The switching

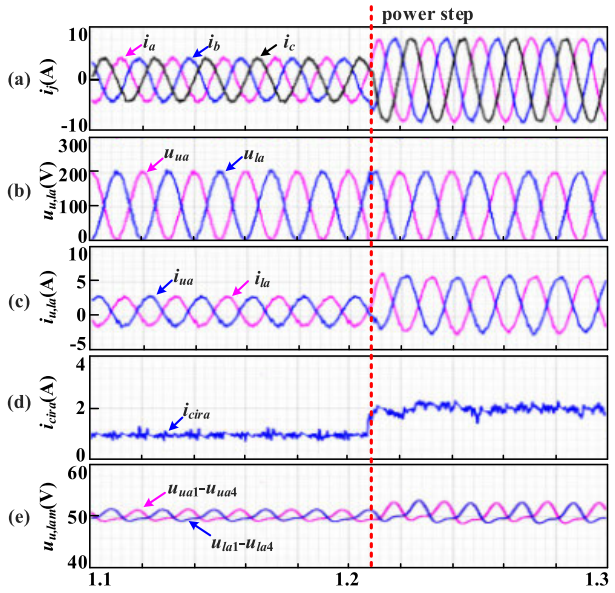


**FIGURE 13.** Experimental results of the power step with the proposed method. (a). Output currents. (b). Output arm voltages. (c). Arm currents. (d). Circulating current. (e). Capacitor voltages.

frequencies of two random SMs ($SM_1$ in the upper arm and $SM_1$ in the lower arm) are shown in Fig. 12, where the frequencies are 2000 Hz. The results verify the effectiveness of the proposed method under steady-state operation.

To further verify the dynamic response of the proposed method, experiments are further carried with a power step. Experimental results are shown in Fig. 13. As shown in Fig. 13 (a), the rated output current increase from 4 A to 8 A at about 1.21 s, where a smooth dynamic response of the output currents is obtained. The output arm voltages of the upper arm and the lower arm in phase A are shown in Fig. 13 (b), the maximum value of which is close to the DC voltage 60 V. And after the power step, a slight increase of the peak-peak value shows in the arm output voltages. Fig. 13 (c) shows the arm currents of the upper arm and the lower arm in phase *A*. At about 1.21 s, the peak-peak value of the arm currents increase, and the DC offset of the arm currents also increase slightly at the same time. The circulating current of phase *A* is shown in Fig. 13 (d), where the circulating current is well suppressed. When the power step occurs, the circulating current increases by about two times and the dynamic response is smooth. The capacitor voltages are shown in Fig. 13 (e), the average value of which is about 50 V during the whole operation. However, at about 1.21 s, the capacitor voltage ripples increase due to the increased output currents. Experimental results verify the proposed method obtains a good dynamic response.

## VI. CONCLUSION

In this paper, a novel SDCS-MMPC scheme is proposed for MMC with a fixed switching frequency in each SM and the reduced computation burden. The main conclusions are described as follows:

1) The proposed MMPC algorithm uses the output voltage references as the basic component control sets. By proper selection of the adaptive search step, only three discrete control sets need to be evaluated in each period. Therefore, the computation burden is significantly reduced.

2) The capacitor voltages between arms are controlled by injecting circulating current. Compared with the MMPC method in [20], the proposed method uses an independent controller to regulate the circulating current. Therefore, the circulating current can better track its reference.

3) Compared with the conventional MPC methods, the proposed method has the superiority of a fixed switching frequency in each SM.

## REFERENCES

[1] G. P. Adam, I. Abdelsalam, J. E. Fletcher, G. Burt, D. Holliday, and S. J. Finney, "New efficient submodule for a modular multilevel converter in multiterminal HVDC networks," *IEEE Trans. Power Electron.*, vol. 32, no. 6, pp. 4258–4278, Jun. 2017.

[2] S. Du, B. Wu, N. R. Zargari, and Z. Cheng, "A flying-capacitor modular multilevel converter for medium-voltage motor drive," *IEEE Trans. Power Electron.*, vol. 32, no. 3, pp. 2081–2089, Mar. 2017.

[3] N. Li, F. Gao, T. Hao, Z. Ma, and C. Zhang, "SOH balancing control method for the MMC battery energy storage system," *IEEE Trans. Ind. Electron.*, vol. 65, no. 8, pp. 6581–6591, Aug. 2018.

[4] B. Fan, Y. Li, K. Wang, Z. Zheng, and L. Xu, "Hierarchical system design and control of an MMC-based power-electronic transformer," *IEEE Trans. Ind. Informat.*, vol. 13, no. 1, pp. 238–247, Feb. 2017.

[5] Q. Yang, M. Saeedifard, and M. A. Perez, "Sliding mode control of the modular multilevel converter," *IEEE Trans. Ind. Electron.*, vol. 66, no. 2, pp. 887–897, Feb. 2019.

[6] J. Qin and M. Saeedifard, "Predictive control of a modular multilevel converter for a back-to-back HVDC system," *IEEE Trans. Power Del.*, vol. 27, no. 3, pp. 1538–1547, Jul. 2012.

[7] J.-W. Moon, J.-S. Gwon, J.-W. Park, D.-W. Kang, and J.-M. Kim, "Model predictive control with a reduced number of considered states in a modular multilevel converter for HVDC system," *IEEE Trans. Power Del.*, vol. 30, no. 2, pp. 608–617, Apr. 2015.

[8] M. Vatani, B. Bahrani, M. Saeedifard, and M. Hovd, "Indirect finite control set model predictive control of modular multilevel converters," *IEEE Trans. Smart Grid*, vol. 6, no. 3, pp. 1520–1529, May 2015.

[9] P. Liu, Y. Wang, W. Cong, and W. Lei, "Grouping-sorting-optimized model predictive control for modular multilevel converter with reduced computational load," *IEEE Trans. Power Electron.*, vol. 31, no. 3, pp. 1896–1907, Mar. 2016.

[10] A. Rashwan, M. A. Sayed, Y. A. Mobarak, G. Shabib, and T. Senjyu, "Predictive controller based on switching state grouping for a modular multilevel converter with reduced computational time," *IEEE Trans. Power Del.*, vol. 32, no. 5, pp. 2189–2198, Oct. 2017.

[11] A. Dekka, B. Wu, V. Yaramasu, and N. R. Zargari, "Dual-stage model predictive control with improved harmonic performance for modular multilevel converter," *IEEE Trans. Ind. Electron.*, vol. 63, no. 10, pp. 6010–6019, Oct. 2016.

[12] P. Guo, Z. He, Y. Yue, Q. Xu, X. Huang, Y. Chen, and A. Luo, "A novel two-stage model predictive control for modular multilevel converter with reduced computation," *IEEE Trans. Ind. Electron.*, vol. 66, no. 3, pp. 2410–2422, Mar. 2019.

[13] Z. Gong, P. Dai, X. Yuan, X. Wu, and G. Guo, "Design and experimental evaluation of fast model predictive control for modular multilevel converters," *IEEE Trans. Ind. Electron.*, vol. 63, no. 6, pp. 3845–3856, Jun. 2016.

[14] J. Huang, B. Yang, F. Guo, Z. Wang, X. Tong, A. Zhang, and J. Xiao, "Priority sorting approach for modular multilevel converter based on simplified model predictive control," *IEEE Trans. Ind. Electron.*, vol. 65, no. 6, pp. 4819–4830, Jun. 2018.

[15] X. Xing, X. Li, F. Gao, C. Qin, and C. Zhang, "Improved space vector modulation technique for neutral-point voltage oscillation and common-mode voltage reduction in three-level inverter," *IEEE Trans. Power Electron.*, vol. 34, no. 9, pp. 8697–8714, Sep. 2019.

[16] A. Dekka, B. Wu, V. Yaramasu, and N. R. Zargari, "Model predictive control with common-mode voltage injection for modular multilevel converter," *IEEE Trans. Power Electron.*, vol. 32, no. 3, pp. 1767–1778, Mar. 2017.
[17] F. Zhang, W. Li, and G. Joós, "A voltage-level-based model predictive control of modular multilevel converter," *IEEE Trans. Ind. Electron.*, vol. 63, no. 8, pp. 5301–5312, Aug. 2016.
[18] B. Gutierrez and S.-S. Kwak, "Modular multilevel converters (MMCs) controlled by model predictive control with reduced calculation burden," *IEEE Trans. Power Electron.*, vol. 33, no. 11, pp. 9176–9187, Nov. 2018.
[19] M. H. Nguyen and S. Kwak, "Simplified indirect model predictive control method for a modular multilevel converter," *IEEE Access*, vol. 6, pp. 62405–62418, 2018.
[20] H. Mahmoudi, M. Aleenejad, and R. Ahmadi, "Modulated model predictive control of modular multilevel converters in VSC-HVDC systems," *IEEE Trans. Power Del.*, vol. 33, no. 5, pp. 2115–2124, Oct. 2018.
[21] D. Zhou, S. Yang, and Y. Tang, "Model-predictive current control of modular multilevel converters with phase-shifted pulsewidth modulation," *IEEE Trans. Ind. Electron.*, vol. 66, no. 6, pp. 4368–4378, Jun. 2019.
[22] J. Wang, Y. Tang, P. Lin, X. Liu, and J. Pou, "Deadbeat predictive current control for modular multilevel converters with enhanced steady-state performance and stability," *IEEE Trans. Power Electron.*, vol. 35, no. 7, pp. 6878–6894, Jul. 2020.
[23] Q. Xiao, L. Chen, H. Jia, P. W. Wheeler, and T. Dragicevic, "Model predictive control for dual active bridge in naval DC microgrids supplying pulsed power loads featuring fast transition and online transformer current minimization," *IEEE Trans. Ind. Electron.*, vol. 67, no. 6, pp. 5197–5203, Jun. 2020.
[24] Q. Xiao, J. Wang, Y. Jin, L. Chen, H. Jia, T. Dragicevic, and R. Teodorescu, "A novel operation scheme for modular multilevel converter with enhanced ride-through capability of submodule faults," *IEEE J. Emerg. Sel. Topics Power Electron.*, early access, Jan. 17, 2020, doi: 10.1109/JESTPE.2020.2967576.
[25] M. Hagiwara and H. Akagi, "Control and experiment of pulsewidth-modulated modular multilevel converters," *IEEE Trans. Power Electron.*, vol. 24, no. 7, pp. 1737–1746, Jul. 2009.
[26] X. Chen, J. Liu, S. Song, S. Ouyang, H. Wu, and Y. Yang, "Modified increased-level model predictive control methods with reduced computation load for modular multilevel converter," *IEEE Trans. Power Electron.*, vol. 34, no. 8, pp. 7310–7325, Aug. 2019.
[27] A. Vidal, F. D. Freijedo, A. G. Yepes, P. Fernandez-Comesana, J. M. O. Lopez, and J. Doval-Gandoy, "A fast, accurate and robust algorithm to detect fundamental and harmonic sequences," in *Proc. IEEE Energy Convers. Congr. Expo.*, Sep. 2010, pp. 1047–1052.

**YU JIN** was born in Heilongjiang, China, in 1994. He received the B.S. degree from the School of Electrical Engineering and Automation, Harbin Institute of Technology, Harbin, China, in 2015, where he is currently pursuing the Ph.D. degree.

Since October 2018, he has been a two-year Visiting Scholar with the Department of Energy Technology, Aalborg University, Aalborg, Denmark. His current research interests include multilevel converters and their applications in FACTS and multi-terminal microgrids, fault diagnosis and fault-tolerant control technique, and advanced control strategies in power converters.

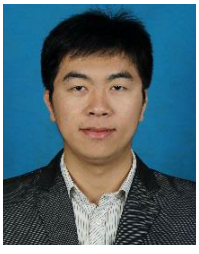

**QIAN XIAO** (Member, IEEE) received the B.S. and M.S. degrees in electrical engineering from the Hebei University of Technology, Tianjin, China, in 2011 and 2014 respectively, and the Ph.D. degree in electrical engineering from Tianjin University, Tianjin, in 2020.

From October 2018 to November 2019, he was a Visiting Scholar with the Department of Energy Technology, Aalborg University, Aalborg, Denmark. Since January 2020, he has been an Assistant Professor with the School of Electrical and Information Engineering, Tianjin University. His research interests include multilevel converters, dc/dc converters, and power electronics for distributed generation, microgrids, and HVDC.

**HONGJIE JIA** (Senior Member, IEEE) received the Ph.D. degree in electrical engineering from Tianjin University, China, in 2001.

He was an Associate Professor with Tianjin University, in 2002, where he was promoted as a Professor, in 2006. His research interests include power reliability assessment, stability analysis and control, distribution network planning and automation, and smart grids.

**YUNFEI MU** (Member, IEEE) was born in Hebei, China. He received the Ph.D. degree from the School of Electrical Engineering and Automation, Tianjin University, Tianjin, China, in 2012.

He is currently an Associate Professor with Tianjin University. His research interests include integrated energy systems, electric vehicles, and smart grids.

**YANCHAO JI** received the B.Eng. and M.Eng. degrees in electrical engineering from Northeast Electric Power University, Jilin, China, in 1983 and 1989, respectively, and the Ph.D. degree in electrical engineering from North China Electric Power University, Beijing, China, in 1993.

He joined the Department of Electrical Engineering, Harbin Institute of Technology, Harbin, China, in 1993. From 1995 to 1996, he was an Associate Professor with the Department of Electrical Engineering, Harbin Institute of Technology, where he is currently a Professor. His current research interests include pulse width modulation technique, power converter, and flexible ac transmission systems devices.

**TOMISLAV DRAGIČEVIĆ** (Senior Member, IEEE) received the M.Sc. and the industrial Ph.D. degrees in electrical engineering from the Faculty of Electrical Engineering, University of Zagreb, Croatia, in 2009 and 2013, respectively. From 2013 to 2016, he was a Postdoctoral Researcher with Aalborg University, Denmark. From 2016 to 2020, he was an Associate Professor with Aalborg University. Since 2020, he has been a Professor with the Technical University of Denmark. He has authored or coauthored more than 200 technical publications (more than 100 of them are published in international journals, mostly in IEEE), eight book chapters, and a book in the field. His research interests include application of advanced control, optimization and artificial intelligence inspired techniques to provide innovative and effective solutions to emerging challenges in design, control and cyber-security of power electronics intensive electrical distributions systems, and microgrids. He serves as an Associate Editor for the IEEE TRANSACTIONS ON INDUSTRIAL ELECTRONICS, the IEEE TRANSACTIONS ON POWER ELECTRONICS, the IEEE EMERGING AND SELECTED TOPICS IN POWER ELECTRONICS, and the *IEEE Industrial Electronics Magazine*.

**REMUS TEODORESCU** (Fellow, IEEE) received the Dipl.Ing. degree in electrical engineering from the Polytechnical University of Bucharest, Romania, in 1989, and the Ph.D. degree in power electronics from the University of Galati, Romania, in 1994.

He joined the Department of Energy Technology, Power Electronics Section, Aalborg University, in 1998, where he currently works as a Professor. From 2013 to 2017, he was a Visiting Professor with Chalmers University. From 2007 to 2013, he was the Coordinator of Vestas Power Program involving ten Ph.D. projects in the areas of power electronics, power systems, and energy storage. He has coauthored the book *Grid Converters for Photovoltaic and Wind Power Systems*, ISBN-10: 0-470-05751-3 – Wiley and over 400 IEEE journals and conference papers. His research interests include design and control of power converters for photovoltaics and wind power systems, grid integration with wind power, HVDC/FACTS-based on MMC, SiC-based converters, and storage systems for utility.

Dr. Teodorescu was the Chair of the IEEE Danish Joint IEEE Industrial Electronics Society, the IEEE Power Electronics Society, and the IEEE Industry Applications Society Chapter. He was an Associate Editor of the IEEE TRANSACTIONS ON POWER ELECTRONICS.

**FREDE BLAABJERG** (Fellow, IEEE) received the Ph.D. degree in electrical engineering from Aalborg University, in 1995. From 1987 to 1988, he was with ABB-Scandia, Randers, Denmark. He was an Assistant Professor, in 1992, an Associate Professor, in 1996, and a Full Professor of power electronics and drives, in 1998.

Since 2017, he has been a Villum Investigator. He is a Honoris Causa with University Politehnica Timisoara (UPT), Romania, and Tallinn Technical University (TTU), Estonia. He has published more than 600 journal articles in the fields of power electronics and its applications. He is the coauthor of four monographs and editor of ten books in power electronics and its applications. His current research interests include power electronics and its applications, such as in wind turbines, PV systems, reliability, harmonics, and adjustable speed drives.

Dr. Blaabjerg has received 30 IEEE Prize Paper Awards, the IEEE PELS Distinguished Service Award, in 2009, the EPE-PEMC Council Award, in 2010, the IEEE William E. Newell Power Electronics Award 2014, the Villum Kann Rasmussen Research Award 2014, and the Global Energy Prize, in 2019. From 2006 to 2012, he was the Editor-in-Chief of the IEEE TRANSACTIONS ON POWER ELECTRONICS. He has been a Distinguished Lecturer of the IEEE Power Electronics Society, from 2005 to 2007, and the IEEE Industry Applications Society, from 2010 to 2011, as well as from 2017 to 2018. From 2019 to 2020, he served the President of the IEEE Power Electronics Society. He is the Vice-President of the Danish Academy of Technical Sciences. He is nominated in 2014-2018 by Thomson Reuters to be between the most 250 cited researchers in Engineering in the world.